Proceedings of the 21st ICSMGE, Vienna, Austria, 14 – 19 June 2026. Pistrol, Adam & Schweiger (eds.)
Published by: ÖGG, Austrian Society for Geomechanics, Salzburg, Austria, ISBN 978-3-9503898-4-5
https://doi.org/10.53243/ICSMGE2026-557

Investigation of natural soil anisotropy using hollow cylinder tests

Abdelilah Errahali, Thibault Badinier, Alain Le Kouby, Aurore Horabik
Univ. Gustave Eiffel, GERS-SRO, F-77454 Marne - la- Vallée, France, abdelilah.errahali@univ-eiffel.fr

Emmanuel Bourgeois
Univ. Gustave Eiffel, COSYS-IMSE, F-77454 Marne-la-Vallée, France

ABSTRACT: Despite the fact that natural soils can exhibit anisotropic behavior, most analytical or numerical models used to predict the soil response (for tunneling for example) still rely on the assumption that soil behavior is isotropic. In these models, the choice of constitutive law for the soil plays a key role. One of the reasons for this simplification lies in the experimental challenges associated with characterizing anisotropy parameters in laboratory tests. However, accounting for anisotropy can significantly improve the accuracy of the predictions. Unlike traditional tests, the Hollow Cylinder Apparatus (HCA), which combines compression and rotation, allows studying anisotropic behaviors and simulating more complex stress paths. The present study demonstrates that the HCA is an effective tool for determining the full set of small-strain anisotropic elastic parameters. A step-by-step methodology based on an analytical study is proposed for experimentally determining these parameters. An application on three reconstituted soil samples is provided, illustrating the test repeatability, the procedure of the proposed approach and analyzing and interpretation of the results. The proposed approach requires a single specimen and does not need horizontal, vertical and/or inclined tests, which are not easy to perform experimentally.

KEYWORDS: Hollow cylinder apparatus, Natural soil anisotropy, Urban tunnel, Stress rotation, Laboratory test.

1 INTRODUCTION

The characterization of the mechanical behavior of natural soils is a fundamental challenge in geotechnical engineering. Many natural soils, especially those of sedimentary origin, exhibit an anisotropic internal structure. (Casagrande & Carillo, 1944) were the first to highlight the importance of soil anisotropy and introduced the concepts of inherent anisotropy and induced anisotropy. The first type is entirely independent of the applied strains and stresses, (Oda & Iwashita, 1999) showed that the preferred orientation and the distribution of contact normal of grains during the sedimentation are the origin of this type of anisotropy. (Casagrande & Carillo, 1944) define the second type, which is the induced anisotropy, as physical characteristic due exclusively "to the strain associated with an applied stress". During the sedimentation process, the vertical axis serves as an axis of radial symmetry. As a result, soils are often assumed to have equal stiffness in all horizontal directions and to exhibit a different stiffness in the vertical direction (Oda, 1972). This type of soil anisotropy is shown as "cross-anisotropic" or "transversely isotropic".

Neglecting the anisotropy of soil behavior may lead to inaccurate prediction of the response. Several numerical studies showed that the small strain stiffness anisotropy can play a non-negligible role in the prediction of settlements induced by tunneling and deep excavations (Lee & Rowe, 1989; Simpson et al., 1996; Addenbrooke et al., 1997; Franzius et al., 2005; Gilleron, 2016; Errahali et al., 2025).

A linear transversely isotropic model can be described by five parameters, namely the vertical and horizontal Young's moduli E_v and E_h, the Poisson's ratio between the vertical and horizontal directions ν_{vh} , the Poisson's ratio in the horizontal plan ν_h , and the shear modulus between the vertical and horizontal directions G_{vh}. The shear modulus in the horizontal plan G_h is not an independent parameter but it is dependent to E_h and ν_h :

$$G_h = \frac{E_h}{2(1+\nu_h)} \quad (1)$$

Determining the anisotropic parameters presents significant challenges. (Graham & Houlsby, 1983) showed that only three parameters : vertical Young modulus and the vertical Poisson's ration and a composite of the horizontal ones could be obtained from conventional triaxial tests, as no pure shear stress can be applied to the sample. Generally, one must test specimens at different orientations relative to the depositional plane (vertical, horizontal, and inclined sample), which presents technical and practical complications. To overcome these limitations, many researchers combine advanced triaxial test with bender element measurement using wave propagation methods to examine these parameters (Gasparre et al., 2007; Yimsiri & Soga, 2011; Ratananikom et al., 2013). However, an important limitation is the differences in the strain levels between the mechanical tests and wave-based measurement, which can lead to some inconsistencies between the determined parameters (Atkinson, 2000; Reiffsteck, 2002).

The Hollow Cylinder Apparatus (HCA) offers a valuable alternative for such investigations. In such a test, the tested sample takes the form of a hollow cylinder, it can be subjected to independent external and internal pressures p_e and p_i respectively, a controlled back pressure BP, an axial load or vertical displacement u_0, and a torque M_t as illustrated in Figure 1. This unique capability allows the simultaneous control of the three principle stresses and can reproduce more complex stress states than triaxial tests. Particularly the produced shear stresses between horizontal and vertical directions make it possible to study intermediate principle stress effects and principals stress rotation occurring around geotechnical structures (Hight et al., 1983; O'Kelly & Naughton, 2005; Reiffsteck & Nasreddine, 2002; Blanc et al., 2011). By exploring the torsional loading mode, the HCA allows direct evaluation of the vertical shear modulus G_{vh} as it will be showed in this paper.

Within a tunneling project for the construction of a new metro-line in Toulouse, new simulation methods are developed with the research project E-PILOT. To evaluate most of the parameters necessary to models, the use of the HCA appeared as the most efficient device. Indeed, the present study demonstrates that the HCA is an effective tool for determining the full set of small-strain anisotropic elastic parameters. A step-by-step methodology based on a previous analytical study is proposed for experimentally determining these parameters.

An application on three reconstituted soil samples is provided, illustrating the test repeatability. The procedure of the proposed approach is described in this paper, along with the analyze and interpretation of the results. The tested samples were reconstituted due to the insufficient external diameter of

the intact soil specimens available. The apparatus used in this study is manufactured by Wille Geotechnik (Germany). The hollow cylindrical specimens had an external diameter of 100 mm, an internal diameter of 60 mm, and a height of 200 mm.

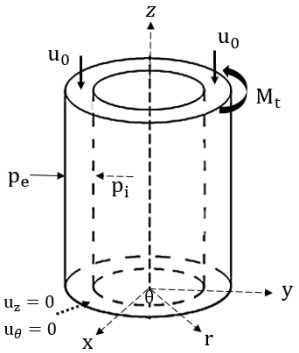

Figure 1: Geometrical configuration and experimental conditions of the hollow cylinder test

2 ANALYTICAL ANALYSIS

A detailed analytical study of the hollow cylinder test on elastic cross-anisotropic soil was carried out (Errahali et al., 2024). The objective of this study was to determine the soil response within the different stages of the test. The relationships between the different types of loadings (torsion, vertical loading, internal and external pressures, etc.) and the measures are then determined.

The analytical study showed that performing vertical shearing permits to determine the vertical Young modulus E_v and the Poisson ratio ν_{vh} in the same direction as the initial slopes of the curves of the deviator stress q (the difference between the vertical stress and the confinement pressure) and the volumetric strain ε_v as functions of the applied vertical strain ε_z:

$$q = E_v \varepsilon_z \tag{2}$$

$$\varepsilon_v = -(1 - 2\nu_{vh})\varepsilon_z \tag{3}$$

These formulas are similar to those used in the conventional triaxial test. At this stage, the confinement (external) pressure must be kept constant and equal to the internal pressure ($p_e = p_i$).

To determine the vertical shear modulus G_{vh}, a rotation θ_t must be applied progressively. In this stage, the deviator stress must be maintained equal to zero to assure an isotropic confinement. The generated torque M_t is measured. The parameter G_{vh} can be calculated as the initial slope using the following equation:

$$M_t = G_{vh} \frac{I}{H} \theta_t \tag{4}$$

In this equation, H is the specimen's height, R_e is its external radius, R_i is its internal radius and $I = \frac{\pi}{2}(R_e^4 - R_i^4)$ is its polar moment of inertia.

At this stage, three of the five seeking parameters are determined, and the horizontal Young modules and the horizontal Poisson ratio are unknown, which means that two other equations are needed.

Combining the equilibrium equation and cross-anisotropic elastic Hooke's law, the radial displacement u_r is obtained for any initial radial distance r (cylindrical coordinate) at the mid-height of the specimen (Errahali et al., 2024):

$$u_r = \frac{A}{r} + Br \tag{5}$$

With A and B as constants calculated using the boundary conditions related to the radial stress at the inner and outer faces of the specimen:

$$A = -\frac{1}{2G_h} \frac{R_e^2 R_i^2}{R_e^2 - R_i^2} (p_e - p_i) \tag{6}$$

$$B = -\left(\frac{1}{2K_h} \frac{R_e^2 p_e - R_i^2 p_i}{R_e^2 - R_i^2} + \nu_{vh} \frac{u_0}{H} \right) \tag{7}$$

Where:

$$K_h = \frac{1}{2} \frac{E_h}{1 - \nu_h - 2\frac{E_h}{E_v}\nu_{vh}^2} \tag{8}$$

The parameter K_h represents a particular form of the soil's volumetric compressibility in the specific case where only horizontal compressibility is permitted (vertical strain being restricted) and $p_e = p_i$ (Errahali et al., 2024). It can be observed that the horizontal shear modulus $G_h = E_h/2(1 + \nu_h)$ is associated to the pressure difference $p_e - p_i$, and the inverse of the radial distance r in the equation (5) . In the case of the conventional triaxial test, the specimen is a solid cylinder, which means that the constant A must be null and in this case, one equation is missing. This means that the five elastic anisotropic parameters cannot all be determined without independently controlling the external pressure and the internal pressure, nor by using a conventional triaxial test as confirmed by (Graham & Houlsby, 1983).

To determine the horizontal shear modulus G_h and the parameter K_h, containing four of the parameters sought, the variations of the mean radius R_m can be used. Blocking the vertical displacement ($u_0 = 0$), this variation can be written taking $r = R_m = (R_e + R_i)/2$ in the equation (5) :

$$\frac{\Delta R_m}{R_m} = -\frac{p_e}{K_e} + \frac{p_i}{K_i} \tag{9}$$

Where we denoted:

$$\frac{1}{K_e} = \frac{2}{1 - \alpha^2} \left(\frac{\alpha}{1 + \alpha} \right)^2 \frac{1}{G_h} + \frac{1}{1 - \alpha^2} \frac{1}{2K_h} \tag{10}$$

$$\frac{1}{K_i} = \frac{2}{1 - \alpha^2} \left(\frac{\alpha}{1 + \alpha} \right)^2 \frac{1}{G_h} + \frac{\alpha^2}{1 - \alpha^2} \frac{1}{2K_h} \tag{11}$$

With $\alpha = R_i/R_e$ is the ratio of the internal and external radii. In the case of a solid specimen, as used in the conventional triaxial test $\alpha = 0$, the term involving G_{hh} vanishes. The mean radial variation can be expressed in function of the variations of the inner and the outer radii as follow:

$$\frac{\Delta R_m}{R_m} = \frac{1}{1 + \alpha} \frac{\Delta R_e}{R_e} + \frac{\alpha}{1 + \alpha} \frac{\Delta R_i}{R_i} \tag{12}$$

Technically, the measurement of variations in the inner radius with sufficient accuracy is challenging; therefore, volumes measured during the test are used instead. In such approximations, the specimen is typically assumed to remain cylindrical. In the present study, a more realistic geometric representation is considered. Considering the horizontal displacement blocked at each extremity of the sample, the radial

displacement is assumed to follow a parabolic distribution along the height of the specimen, reaching its maximum at mid-height and becoming zero at the upper and lower boundaries. Therefore, a method is proposed in which the variations of the sample volume V_s and the hollow volume V_h measured during the test are employed. During this stage, the vertical displacement is restricted as previously mentioned, only the pressures p_e and p_i are varied and influence the horizontal displacement. Under these assumptions, the following expressions were obtained for the variations of the internal and external radii:

$$\frac{\Delta R_i}{R_i} = \frac{5}{4}\left(\sqrt{1+\frac{6}{5}\frac{\Delta V_h}{V_{h0}}}-1\right) \quad (13)$$

$$\frac{\Delta R_e}{R_e} = \frac{5}{4}\left(\sqrt{1+\frac{6}{5}\left(\alpha^2\frac{\Delta V_h}{V_{h0}}+(1-\alpha^2)\frac{\Delta V_s}{V_{s0}}\right)}-1\right) \quad (14)$$

Where V_{h0} and V_{s0} are the initial hollow and sample's volumes respectively. By varying p_e and p_i independently and measuring the mean radius variations, one can evaluate K_e and K_i. Then, one can obtain G_h and K_h as follows:

$$G_h = 2\left(\frac{\alpha}{1+\alpha}\right)^2\frac{K_e K_i}{K_e-\alpha^2 K_i} \quad (15)$$

$$K_h = \frac{1}{2}\frac{K_i K_e}{K_i-K_e} \quad (16)$$

These expressions imply that the ratio K_e/K_i must be greater than α^2 and less than one. Based on the parameters determined, the horizontal modulus E_h and Poisson's ratio ν_h can be calculated as follow:

$$\nu_h = \frac{1-2G_h\left(\frac{1}{2K_h}+\frac{2\nu_{vh}^2}{E_v}\right)}{1+2G_h\left(\frac{1}{2K_h}+\frac{2\nu_{vh}^2}{E_v}\right)} \quad (17)$$

$$E_h = 2(1+\nu_h)G_h \quad (18)$$

3 EXPERIMENTAL PROCEDURE

In this section, the proposed methodology is applied to a natural soil extracted from a site in Toulouse, France, at a depth of 18 meters. It is classified as silty sand (SM) according to the Unified Soil Classification System (USCS), 50% sand, 49% silt and 1% clay with an in-situ dry density of 19kN/m^3 and a natural water content of 15%. Three hollow cylinder tests were performed on reconstituted soil samples build to match the same initial properties.

To reproduce the relatively high natural density, static compaction was carried out using a hydraulic press with a maximum capacity of 50 kN. The difference between the three samples is mainly the used compaction method. The first sample named hereafter “Test 1” is “single-sided compacted”. In that case, the desired soil mass is poured at in the cylindrical mold in one layer and pressed at its top side until the target height of 200 mm is reached. The second test named “Test 2” is “double-sided compacted” which means that the soil is compacted alternatively at the two sides of the sample until the target height. The third test named “Test 3” is compacted in 10 successive layers. In that case, the soil mass is divided in 10 and each layer is compacted to reach the target height of 20mm for a total height of 200mm of the specimen. For each sample, the hole in the solid samples is formed manually and progressively using three helical shafts of different diameters (Figure 2). This procedure is inspired by the method described by (Reiffsteck et al., 2007).

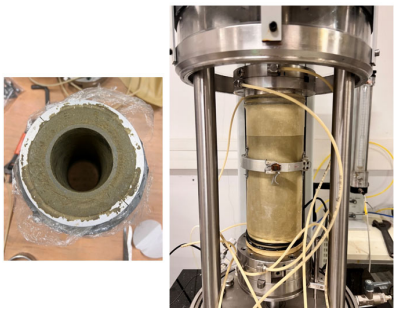

Figure 2: Sample preparation and installation

Similar to the conventional triaxial test, the hollow cylinder test begins with a saturation phase. During this phase, a back pressure is applied in order to inject water into the soil. Higher cell pressure is applied around the soil to prevent any risk of swelling; the effective pressure (the difference between the two pressures) must remain below the consolidation pressure. The back pressure is applied gradually, step by step (200 kPa, 300 kPa, etc.) and relatively slowly. At the end of each step, saturation is checked using Skempton's B ratio, which measures the ratio of the pore pressure generated in the sample, under undrained conditions, by an increment of confining pressure (e.g. 50 kPa). Once the sample is saturated, the consolidation phase begins. During this phase, the back pressure is maintained at the value of the last saturation step and the cell pressure is increased until the desired effective pressure is reached (250 kPa in this study). During the consolidation phase, the deviator stress (the difference between the vertical stress and the cell pressure) must be maintained at a minimum value ensuring contact and isotropic consolidation. Under consolidation stress, the volume of the sample decreases over time and tends towards an asymptotic direction with a low slope. During the saturation and consolidation phases, the internal and external pressures are maintained equal $p_e = p_i$.

The next stage involves applying a radial pressure difference ($p_e - p_i \neq 0$). In accordance with the analytical study, vertical displacement is restricted ($u_0 = 0$) by fixing both the top and bottom bases. The cell pressure (external pressure p_e) is controlled independently from the hollow pressure (internal pressure p_i). A 30 kPa increment of internal pressure is first applied, followed by unloading back to the consolidation stress. The internal pressure is then kept constant while a 30 kPa increment of external cell pressure is applied, after which unloading is carried out to return to the consolidation pressure. All pressure increments are applied at a rate of 1 kPa/min to ensure drained conditions.

Next, isotropic consolidation conditions are restored (vertical displacement released and deviator stress maintained at its minimum contact value), and a torsion test is performed; At a speed of 0.1°/min, a rotation of 0.6°, corresponding to a distortion value of 0.21%, is applied, followed by an unloading-loading cycle (not presented in this paper). Finally, vertical loading until failure is performed at a speed of 0.1mm/min.

4 RESULTS

This section presents the obtained results. The logic of the method developed requires starting with an analysis of the last phase, which is the vertical shear phase, in order to determine the vertical Young's modulus E_v and the vertical Poisson's ratio ν_{vh}.

4.1 *Vertical Young modulus and vertical Poisson's ratio*

Figure 3 shows the evolution of the deviator stress q (difference between the vertical stress and the radial stress) as a function of the applied axial strain ε_z. A satisfactory repeatability is obtained, especially at the small strain levels. The different response observed in 'Test 1' may be attributed to the sample compaction method. In this case, the sample was compacted from one side, which can lead to non-uniform density along its height.

Figure 4 shows, on a semi-logarithmic scale, the vertical tangent Young modulus E_v obtained using the equation (2). The results exposed typical modulus degradation with increasing strain as observed by many other studies (Atkinson, 2000; Reiffsteck, 2002). This study focuses on the small strain level, the maximal vertical Young modulus of the three tests is presented in Table 1 . The mean value is 135 MPa.

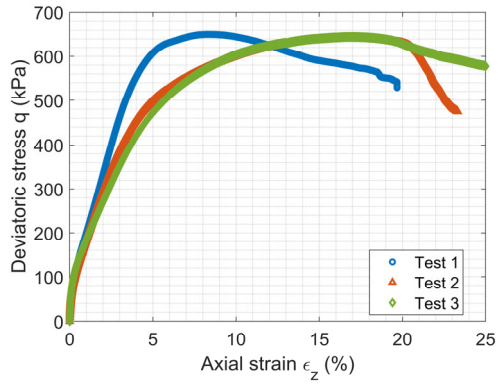

Figure 3: deviator stress as function of the axial strain during the vertical shearing phase

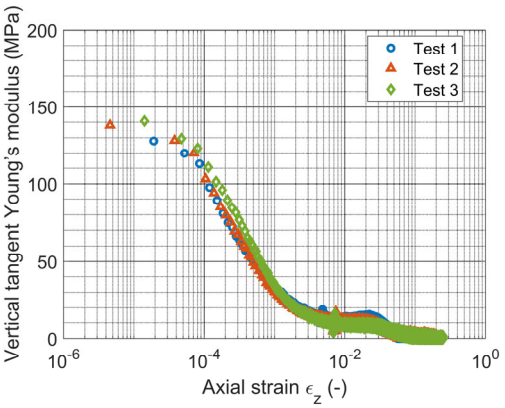

Figure 4 : Vertical tangent Young modulus as function of axial strain

Table 1: Vertical Young modulus

Test	Test 1	Test 2	Test 3	Mean value
E_v (MPa)	128	138	141	135

Figure 5 shows the variation in volumetric strain ε_v (Variation of the sample volume divided by the initial volume) as a function of axial strain ε_z. All the specimens exhibit dilatant behavior at large strain levels, in accordance with the expected response of a dense sand.

At small strain, with assumed elastic behavior, ν_{vh} is evaluated using the equation (3). The obtained results are presented in Table 2. The mean value is 0.44.

Table 2: Vertical Poisson ratio

Test	Test 1	Test 2	Test 3	Mean value
$\frac{\Delta\varepsilon_V}{\Delta\varepsilon_z}$	-0.139	-0.115	-0.083	-0.112
ν_{vh}	0.43	0.44	0.45	0.44

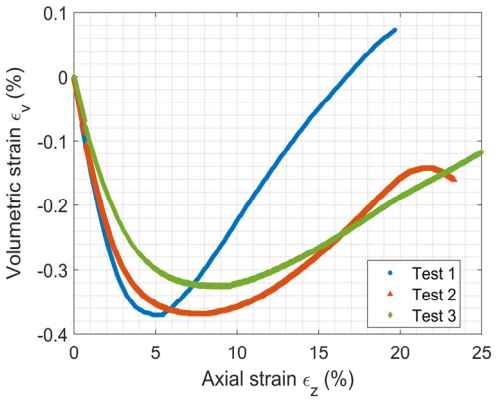

Figure 5: Volumetric strain as function of axial strain during the vertical shearing phase

4.2 *Horizontal Young modulus and horizontal Poisson ratio*

Using equations (13) and (14) , one can evaluate the variation of the internal radius and external radius of the sample from sample and hollow volume measures, and deduce the mean radius variation due to the applied internal pressure p_i and the external pressure p_e using the equation (12).

These variations are represented in the Figure 6. Obviously, the internal pressure tend to increase the mean radius and its variations are then positive values, whereas the external pressure tend to reduce the mean radius so the variations are negatives, which is in line with obtained results. In addition, a quasi-linear behavior is observed for the Test 3, with pronounced plastic strains particularly in Test 1 and 2. To evaluate the constrained compressibilities K_e and K_i defined by the equations (9), (10) and (11), the initial slopes are considered in order to approximate the elastic domain as closely as possible (Figure 6). Once the values of K_e and K_i are known, one can calculate the horizontal shear modulus G_h and the constrained horizontal compressibility K_h using the equations (15) and (16). Once these two parameters are determined, one can evaluate the horizontal Young modulus E_h and the horizontal Poisson's ratio ν_h directly using equations (17) and (18) respectively. The obtained values are presented in Table 3.

Table 3: Constrained compressibilities, horizontal shear and Young's moduli, and horizontal Poisson ratio

Test	K_i (MPa)	K_e (MPa)	K_h (MPa)	G_h (MPa)	E_h (MPa)	ν_h
Test 1	55.28	42.16	88.79	29.45	78.43	0.33
Test 2	56.15	40.12	70.29	31.82	78.02	0.22
Test 3	53.99	42.56	100.56	27.94	77.70	0.39
Mean values	55.14	41.61	86.54	29.73	78.05	0.31

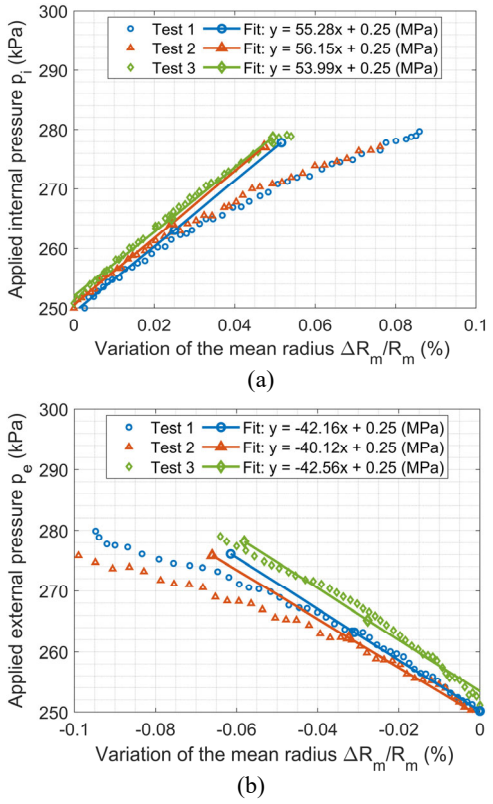

Figure 6: Variations in the mean radius of the sample due to the internal pressure (a) and the external pressure (b)

The vertical shear modulus G_{vh} is determined in the next section.

4.3 *Vertical shear modulus*

Figure 7.a shows the measured torque caused by the applied rotation; the tangent vertical shear modulus obtained from the equation (4) is represented in the Figure 7.b as function of the shear strain γ calculated at the mean radius using the following geometric formula:

$$\gamma \cdot H = \theta_t \cdot \frac{R_i + R_e}{2} \qquad (19)$$

Again, typical shear modulus degradation with increasing strain is observed (Atkinson, 2000; Reiffsteck, 2002). Similarly to the other parameters, G_{vh} is evaluated at small strain level. The obtained results are presented in Table 4.

Table 4: Vertical shear modulus

Test	Test 1	Test 2	Test 3	Mean value
G_{vh} (MPa)	43.87	38.51	40.79	41.05

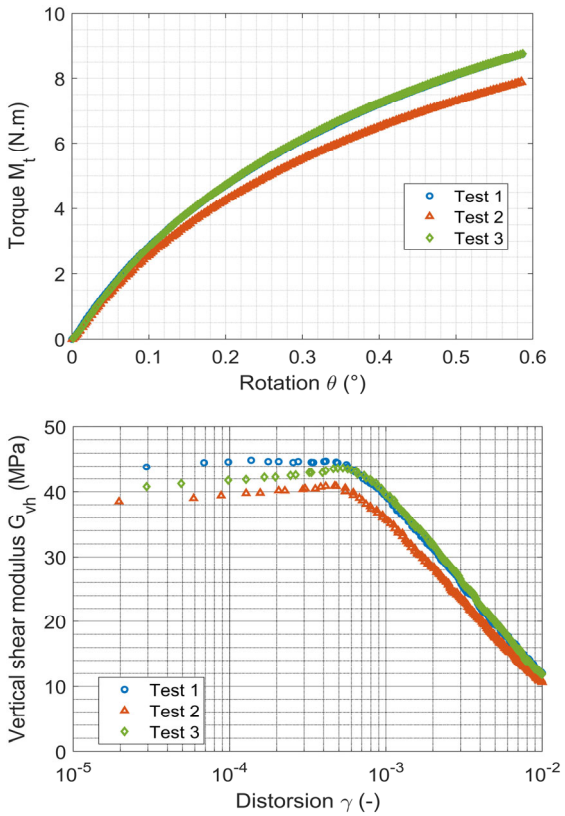

Figure 7 : (a) Soil response to the torsional loading (b) Degradation of vertical tangent shear modulus as function of the distortion

5 DISCUSSION

The results of this study confirm that the hollow cylinder test is a suitable and reliable technique for investigating the anisotropic elastic behavior of soils considered as linear-elastic and transversely isotropic. The experimental protocol developed here covers all stages of the laboratory workflow, from sample preparation to data analysis, and includes sequential loading paths specifically designed to identify the five independent elastic parameters characterizing transverse isotropy.

In this work, the specimens were reconstituted. Nevertheless, the same methodology remains applicable to both intact and reconstituted soils. The anisotropy observed in the tests is therefore attributed to inherent anisotropy, reflecting particle arrangement induced during sample preparation or sedimentation processes. Since consolidation was performed under isotropic stress conditions, no significant stress-induced anisotropy is expected, in line with previous findings on the minimal impact of isotropic consolidation on directional stiffness (Oda et al., 1985).

The mechanical parameters obtained show pronounced stiffness anisotropy at small strains. The vertical Young's modulus is significantly higher than the horizontal one (ratio ≈ 1.73), the vertical shear modulus also exceeds the horizontal one (ratio ≈ 1.36), and the vertical Poisson's ratio is greater than the horizontal (ratio ≈ 1.41). These trends are consistent with the specimen preparation method: vertical static compaction may promote a preferential vertical alignment of grains, increasing stiffness along the vertical direction. This behavior is comparable to some sedimentary sandy soils where geostatic stresses induce vertically oriented structures. Conversely, other

natural soils—particularly clays—may display the opposite trend. For example, plate-like clay particles, such as those in London Clay, commonly align horizontally during sedimentation, resulting in higher horizontal stiffness (Gasparre, 2007; Graham & Houlsby, 1983).

6 CONCLUSIONS AND PERSPECTIVES

This study demonstrates that the hollow cylinder test provides an effective framework for quantifying elastic anisotropy in soils and for determining the full set of elastic constants associated with transverse isotropy. The experimental program carried out on reconstituted silty sand compacted using three different procedures highlights clear anisotropic stiffness behavior.

The methodology developed here lays the groundwork for future investigations. Upcoming work will focus on applying this testing procedure to additional soil types, including the Toulouse (France) case-study soil. The results will be used to calibrate numerical models for tunnel excavation. By integrating anisotropic stiffness parameters into these models, it will become possible to evaluate their influence on predicted ground deformation patterns, especially the settlements induced by tunnel boring machine (TBM) advancement.

7 ACKNOWLEDGEMENTS

Results presented in this paper have been obtained within the framework of the French research Project E-PILOT (Evaluation of the impact on PILes response during Tunnelling) ANR-21-CE22-0011.

E-PILOT is a joint industry project dedicated to the behavior of piles during Tunneling. The project, driven by University Gustave Eiffel involves 4 contracting or consulting companies of the civil engineering sector, 2 contracting authorities and 4 universities and research laboratories. The project is funded by the partners, ANR and MTE.

The authors are indebted to the partners for granting permission to publish the results.

8 REFERENCES

Addenbrooke, T., Potts, D., & Puzrin, A. (1997). The influence of pre-failure soirl stiffness on the numerical analysis of tunnel construction. Géotechnique, 47(3), 693-712.

Atkinson, J.H. and Sallfors, G. (1991) Experimental Determination of Soil Properties. Proceedings of the 10th ECSMFE, Vol. 3, 915-956.

Blanc, M., Di Benedetto, H., & Tiouajni, S. (2011). Deformation characteristics of dry Hostun sand with principal stress axes rotation. Soils and Foundations, 51(4), 749–762. https://doi.org/10.3208/sandf.51.749

Casagrande, A., & Carrillo, N. (1944). Shear Failure of Anisotropic Materials. Proceedings of the Boston Society of Civil Engineers, **31**(4), 74–87.

Errahali, A., Bourgeois, E., Badinier, T., & Le Kouby, A. (2024). Modelling a hollow cylinder test on an anisotropic soil. Journées Nationales de Géotechnique et de Géologie de l'Ingénieur (JNGG 2024), Poitiers, France.

Errahali, A., Bourgeois, E., Badinier, T., & Le Kouby, A. (2025). The impact of soil anisotropy on surface settlements induced by tunnelling: A revealing parametric study and nomogram development to improve modelling practice. International Journal for Numerical and Analytical Methods in Geomechanics. https://doi.org/10.1002/nag.70158

Franzius, J., Potts, D., & Burland, J. (2005). The influence of soil anisotropy and K0 on ground surface movements resulting from tunnel excavation. Géotechnique, 55(3), 189-199.

Gasparre, A., Nishimura, S., Minh, N. A., Coop, M. R., & Jardine, R. J. (2007). The stiffness of natural London Clay. Géotechnique, 57(1), 33–47. https://doi.org/10.1680/geot.2007.57.1.33

Gilleron, N. (2016). Méthode de prévision des tassements provoqués par le creusement des tunnels urbains et influence des présoutènements (PhD thesis, Université Paris Est). [In French]

Graham, J., & Houlsby, G. (1983). Anisotropic elasticity of a natural clay. Géotechnique, 33(2), 165-180.

Hight, D. W., Gens, A., & Symes, M. J. (1983). The development of a new hollow cylinder apparatus for investigating the effects of principal stress rotation in soils. Géotechnique, 33(4), 355–383. https://doi.org/10.1680/geot.1983.33.4.355

Lee, K., & Rowe, R. (1989). Deformations caused by surface loading and tunnelling : the role of elastic anisotropy. Géotechnique, 39(1), 125-140.

Oda, M. (1972). Initial fabric and its effect on the mechanical behavior of soils. Géotechnique,22(3),173–187.

Oda, M. and Iwashita K., (1999), 'Mechanics of granular materials: an introduction', Balkema, Rotterdam/Brookfield.

Oda, M., Nemat-Nasser, S., and Konishi, J. (1985). Stress-induced anisotropy in granular masses. Soils Found., 25(3), 85-97.

Reiffsteck, P. (2002). Nouvelles technologies d'essai en mécanique des sols. Etat de l'art. Symp. Int RARAM 2002, Paris, 201-242. [In French]

Reiffsteck, P., & Nasreddine, K. (2002). Cylindre creux et détermination de paramètres de lois de comportement des sols. Symp. Int PARAM 2002, Paris. [In French]

Reiffsteck, P., Tacita, J.-L., Mestat, P., & Pilnière, F. (2007). La presse triaxiale pour éprouvettes cylindriques creuses du LCPC adaptée à l'étude des sols naturels. Bulletin des Laboratoires des Ponts et Chaussées, (270-271), 109-131. [In French]

Ratananikom, W., Likitlersuang, S., & Leroueil, S. (2013). An investigation of anisotropic elastic parameters of Bangkok Clay from vertical and horizontal cut specimens. Geomechanics and Geoengineering, 8(1), 15–29.

Simpson, B., Atkinson, J., & Jovicic, V. (1996). The influence of anisotropy on calculations of ground settlements above tunnels. Proceeding, International symposium on geotechnical aspects of underground construction in soft ground, 591-596.

Yimsiri, S., & Soga, K. (2011). Cross-anisotropic elastic parameters of two natural stiff clays. Géotechnique, 61(9), 809–814.